

- [22] A. Charnes and W. W. Cooper, "Programming with linear fractional functionals," *Naval Res. Logist. Quarter*, vol. 9, no. 3/4, pp. 181–186, Sep./Dec. 1962.
- [23] W. Ai, Y. Huang, and S. Zhang, "New results on Hermitian matrix rank-one decomposition," *Math. Program.*, vol. 128, no. 1/2, pp. 253–283, Jun. 2011.
- [24] A. Ben-Tal and A. Nemirovski, *Lectures on Modern Convex Optimization: Analysis, Algorithms, and Engineering Applications*. Philadelphia, PA, USA: SIAM, 2001.

PRADA: Prioritized Random Access With Dynamic Access Barring for MTC in 3GPP LTE-A Networks

Tzu-Ming Lin, Chia-Han Lee, *Member, IEEE*, Jen-Po Cheng,
and Wen-Tsuen Chen, *Fellow, IEEE*

Abstract—Due to the huge amount of machine-type communications (MTC) devices, radio access network (RAN) overload is a critical issue in cellular-based MTC. The prioritized random access with dynamic access barring (PRADA) framework was proposed to efficiently tackle the RAN overload problem and provide quality of service (QoS) for different classes of MTC devices in Third-Generation Partnership Project (3GPP) Long-Term Evolution Advanced (LTE-A) networks. The RAN overload issue is solved by preallocating random access channel (RACH) resources for different MTC classes with class-dependent back-off procedures and preventing a large number of simultaneous random access requests using dynamic access barring. In this paper, the performances of LTE-A without access barring, extended access barring (EAB), and PRADA are mathematically derived and compared, showing the superior performance of the PRADA scheme.

Index Terms—Access barring, long-term evolution-A (LTE-A), machine-to-machine (M2M), machine-type communication (MTC), random access network (RAN).

I. INTRODUCTION

Machine-type communications (MTC) or machine-to-machine communications emerge to achieve ubiquitous and automatic communication among devices without any human intervention. MTC devices are connected through networks and the Internet to form the so-called Internet of Things [1], enabling a wide range of applications in domains spanning domotics [2], e-health [3], smart grid [4], etc. Cellular systems are expected to play a major role in the successful deployment of MTC devices due to the benefits of widely deployed infrastructures and the support of long-range high-mobility communications [5]–[7]. In particular, the Third-Generation Partnership Project (3GPP) Long-Term Evolution Advanced (LTE-A) has been regarded

as a promising system for facilitating MTC. However, one major challenge that the deployment of MTC over cellular networks faces is the radio access network (RAN) overload issue. Current cellular networks are designed for human-to-human (H2H) communications, and LTE-A, in particular, is designed for broadband high-data-rate applications, whereas most MTC devices transmit and receive a small amount of data. Moreover, the number of MTC devices is expected to be much larger than that of H2H communications in the near future, to reach a number ranging from billions to trillions [1], [8]. Thus, the deployment of massive MTC devices will generate a huge amount of signaling and data, yielding congestion of RAN and core network. Among the 3GPP proposals for solving this issue, extended access barring (EAB) is considered the most efficient scheme to control the potential surge of access requests [9]. Nevertheless, EAB lacks a mechanism to determine the timing of activation and the parameters to use, leading to unsatisfactory performance. Therefore, the prioritized random access with dynamic access barring (PRADA) framework [10] was proposed to efficiently tackle the overload problem for MTC operating under 3GPP LTE-A networks.

In this paper, the PRADA scheme is analyzed. The access success probabilities of LTE-A without access barring, with EAB, and by applying PRADA are mathematically analyzed. Comparing with the simulation results confirms the accuracy of the theoretical analyses.

The rest of this paper is organized as follows. The PRADA framework is reviewed in Section II. Performances of EAB and PRADA are analyzed in Section III and numerically compared in Section IV. Finally, Section V concludes this paper.

II. PRIORITIZED RANDOM ACCESS WITH DYNAMIC ACCESS BARRING FRAMEWORK

Prior to sending data, a user equipment (UE) gets attention of the eNB through the physical random access channel (PRACH), which carries the random access preamble. PRACH occupies several resource blocks in the frequency domain and appears every several subframes, depending on the configuration. The UE then requests for radio resources by a four-step random access (RA) procedure: random access preamble selection and transmission (called Msg1), random access response (RAR), connection request, and contention resolution [10], [11]. A collision is detected by UEs if RAR is not received within the RA response window. This happens if two or more UEs select the same preamble such that the eNB is unable to decode any of the preambles and does not send RAR. Since the number of preambles is limited, a large amount of UEs would have a high probability of selecting the same preambles. Without the unique preamble selection, a UE cannot be granted access and has to repeat the random access procedure. Thus, UEs may experience low access success rate and significant access delay if the number of UEs is huge.

The PRADA framework solves the RAN overload problem by preallocating PRACH resources for different MTC classes while preventing a large number of simultaneous random access requests. The PRADA framework is composed of two core components: virtual resource allocation with class-dependent back-off procedures and dynamic access barring (DAB). To guarantee quality of service, traffic is classified into five categories: emergency, H2H, high priority, low priority, and scheduled [10]. According to the traffic classification, PRADA preassigns different amount of PRACH slots for different classes. The PRACH slots allocated to a specific class is called the *virtual resource* for that class. The physical resource is the PRACHs allocated by eNB, whereas the virtual resource represents the specific PRACHs that can be used for each class. Virtual resources are assigned to different kinds of traffic according to the rules specified in [10].

Manuscript received March 21, 2013; revised June 12, 2013, August 16, 2013, and October 9, 2013; accepted October 17, 2013. Date of publication January 23, 2014; date of current version June 12, 2014. The review of this paper was coordinated by Dr. W. Song.

T.-M. Lin is with the Information and Communications Research Laboratories, Industrial Technology Research Institute, Hsinchu 31040, Taiwan, and also with the Institute of Communication Engineering, National Tsing Hua University, Hsinchu 300, Taiwan.

C.-H. Lee and J.-P. Cheng are with the Research Center for Information Technology Innovation, Academia Sinica, Taipei 115, Taiwan.

W.-T. Chen is with the Institute of Information Science, Academia Sinica, Taipei 115, Taiwan, and also with the Institute of Communication Engineering, National Tsing Hua University, Hsinchu 300, Taiwan.

Color versions of one or more of the figures in this paper are available online at <http://ieeexplore.ieee.org>.

Digital Object Identifier 10.1109/TVT.2013.2290128

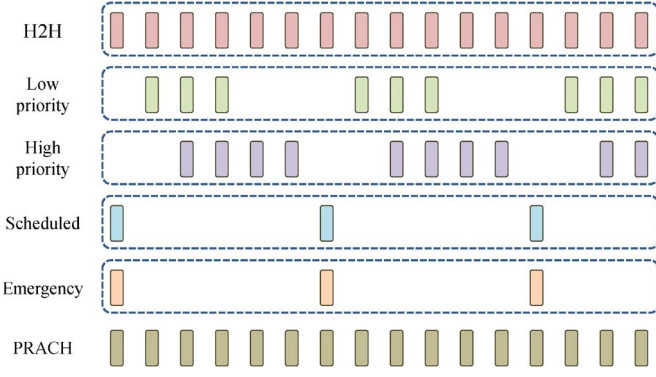


Fig. 1. Virtual resource allocation for five classes of traffic. PRACH appears every several subframes, depending on the system configuration.

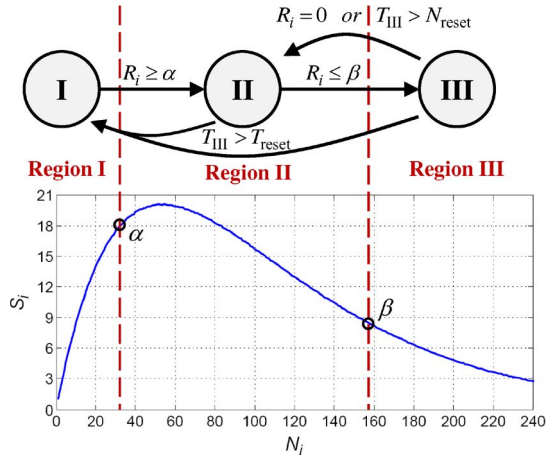


Fig. 2. State transition diagram with the enabling/disabling mechanism in DAB. N_i is the total amount of RA requests during the i th PRACH slot, and S_i is the expected number of successfully decoded Msg1 during the i th PRACH slot. T_{III} denotes the total time spent in states II and III, T_{reset} is the time to reset DAB, and $R_i = (S_i + S_{i-1})/2$. Adapted from [10].

As shown in Fig. 1, for example, emergency and scheduled classes are allocated one virtual resource for every six PRACHs (physical resource); for the class of low priority, the second, third, and fourth PRACHs are allocated as its virtual resource.

Although different resources have been allocated for different classes to reduce the chance of collision, the number of MTC devices can be too large for eNB to grant enough number of channel access requests in a short time. To overcome the bursty traffic, DAB is proposed to reshape and distribute the traffic [10]. To help describe the details of DAB, let $N_{i,k}$ be the number of RA requests that have transmitted Msg1 k times until the i th PRACH slot, and let L be the given maximum number of retransmissions. The total amount of RA requests during the i th PRACH slot can be expressed by $N_i = \sum_{k=0}^{L+1} N_{i,k}$. Then S_i , the expected number of successfully decoded Msg1 transmissions during the i th PRACH slot, is a function of N_i (as shown in Fig. 2) and used by eNB as the loading indicator. DAB operates as follows. eNB continuously monitors S_i to determine the state of the current loading by using the state transition diagram shown in Fig. 2. Let $R_i = (S_i + S_{i-1})/2$. Starting from state I (low traffic loading), the loading state transits to state II (medium loading) when eNB observes $R_i \geq \alpha$ and further transits to state III (high loading) if it becomes $R_i \leq \beta$, where α and β are thresholds for system design. eNB marks a high-loading flag in the system information blocks to 1 (the default is 0) to activate access barring if and only if the current loading is high (in state III). This forces MTC devices transmitting for

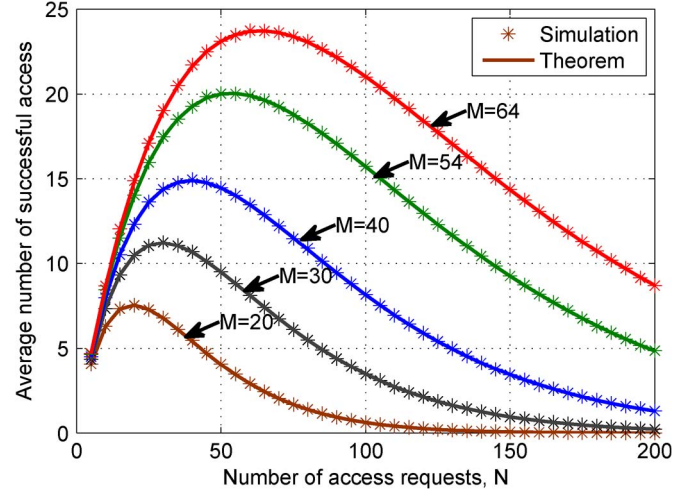


Fig. 3. Average number of successful access versus number of access requests under various preamble numbers.

the first time to delay their access requests for time T_1 , thus reducing N_i . DAB is disabled (the flag is reset to 0) when one of the three conditions is satisfied: After staying in state III for N_{reset} slots, $R_i = 0$ is observed, or the total time staying in states II and III is more than T_{reset} . To further handle the worst-case RAN overload, if having not transmitted Msg1 for more than T_{extra} , an MTC device transmitting for the first time delays its access request for time T_2 , where $T_2 \gg T_1$. Note that as shown in Fig. 2, S_i can correspond to two N_i values. To resolve this, if eNB detects an increase in S_i when N_i is expected to increase, it knows that the S_i corresponds to the smaller N_i ; if detecting a decrease in S_i , the S_i corresponds to the larger N_i .

III. THEORETICAL ANALYSIS OF THE ACCESS SUCCESS PROBABILITY

Here, we derive the access success probabilities of LTE-A without access barring, EAB, and PRADA. The access success probability is defined as the probability of successful completion of the RA procedure within the maximum number of Msg1 transmissions. This is equivalent to the probability that a UE can select a unique preamble within the maximum number of trials, which is closely equivalent to the probability that the number of requests is below the system capacity when a UE performs random access. This approximation is found to work well, as will be explained and shown later. During the derivation, we assume that the number of devices in the category of scheduled traffic is the largest among all classes of UEs, and we ignore the case of unsuccessful retransmissions.

A. System Capacity

We begin with deriving the system capacity. It can be obtained (see the Appendix) that the expected number of successful RA requests per PRACH slot is $N(1 - 1/M)^{N-1}$ for N RA requests and M preambles and is maximized when $\hat{N} = [\log(M/(M-1))]^{-1}$ (see Fig. 3). Therefore, the maximum expected number of successful RA requests per PRACH slot (the capacity per PRACH slot) is

$$c = \left[\log \left(\frac{M}{M-1} \right) \right]^{-1} \left(1 - \frac{1}{M} \right)^{\left[\log \left(\frac{M}{M-1} \right) \right]^{-1} - 1}. \quad (1)$$

The system capacity per second C can then be derived as $C = c \times N_{RACH}$, where N_{RACH} is the number of PRACHs per second.

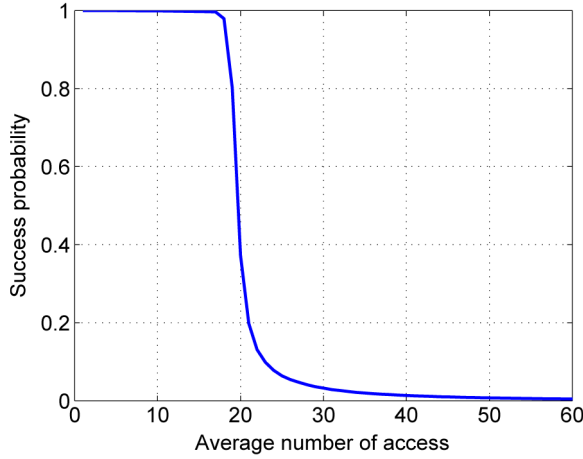


Fig. 4. Success probability versus average number of access requests per PRACH slot (by simulations). The number of preambles is 54.

B. LTE-A Without Access Barring

To derive the access success probabilities, first, let us consider the case of LTE-A without access barring. The RA requests of H2H, emergency, low priority, and high priority will succeed when no RA requests from scheduled devices appear if RA requests per second $\lambda_v + \lambda_e + \lambda_l + \lambda_h$ is smaller than the system capacity, where λ_v , λ_e , λ_l , and λ_h are random access requests per second for H2H, emergency, low-priority, and high-priority traffic, respectively. Note that the following derivations are based on this condition. In the analysis of this paper, we assume that the steps 2–4 in the LTE-A random access procedure [10], [11] between UE and eNB are successful (maybe after retransmissions). We regard the main reason for access failure to be the difficulty of selecting a unique preamble when a large number of access requests happen simultaneously. If a UE cannot select a unique preamble, it can try again after the back off. With the back-off mechanism, the random access of UE can, in general, be successful when the total number of access requests is lower than the system capacity. The bottleneck of the current MTC system is thus mainly at the number of MTC devices. As a result, if the scheduled traffic, which is assumed to be the major MTC traffic, does not appear, other types of traffic can access successfully. Note that an access request may be unsuccessful even when the total number of access requests is less than the capacity, as shown in Fig. 4. However, for theoretical analysis, we can approximate the system performance by assuming that the system capacity serves as the threshold for success and failure of RA requests. Another concern is that the transmissions in steps 3 and 4 might be unsuccessful even after retransmissions, which results in overestimating the RA success probability. This is neglected in our analysis due to little performance degradation.

Let $P_{\text{LTE},v}$, $P_{\text{LTE},e}$, $P_{\text{LTE},l}$, and $P_{\text{LTE},h}$ be access the success probabilities of H2H, emergency, low-priority, and high-priority traffic, respectively. The above probabilities of access success are thus lower bounded by the probability that the scheduled traffic does not appear. Therefore

$$\begin{aligned} P_{\text{LTE},v} = P_{\text{LTE},e} = P_{\text{LTE},l} = P_{\text{LTE},h} \\ > P_{\text{LTE},\text{bound}} = 1 - \frac{\delta_s}{\tau_s} \end{aligned} \quad (2)$$

where τ_s and δ_s are the traffic cycle and the synchronization range for the scheduled traffic, respectively. The *traffic cycle* represents how often a burst of traffic comes. During the traffic cycle, the random access request of a UE is assumed to happen once. The *synchronization range* is the period the traffic distributes, i.e., the time period between

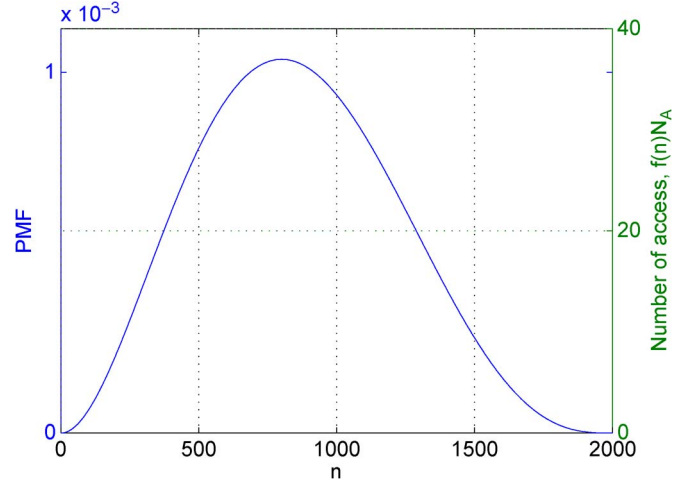


Fig. 5. Example of $f(n)$. Note that n only takes integer values. $f(n)N_A$ is also shown with the right y -axis. $N_A = 35\,670$.

the first and the last RA requests in that burst for a class of traffic. For example, if the traffic cycle is 5 min and the synchronization range is 10 s for a class of UE, the random access request of a UE happens at a random time during the first 5 min, and it will not happen again until the next 5 min. In addition, the first and the last access requests within that 5-min period are not apart for more than 10 s.

Equation (2) is explained as follows. On average, an RA request cooccurs with the requests of scheduled traffic with probability δ_s/τ_s . This is because the burst of the scheduled traffic lasts for δ_s seconds for every τ_s seconds. When cooccurring with the scheduled traffic, the RA request assumes to fail due to the large number of requests from the scheduled traffic. On the other hand, when not cooccurring with the scheduled traffic (with probability $1 - \delta_s/\tau_s$), the access request is assumed to succeed.

A more accurate estimation is possible. Until now, we assume that the random access requests of emergency, H2H, high priority, or low priority will fail when the large amount of requests from the scheduled devices appears. In fact, RA requests of emergency, H2H, high priority, or low priority have chance (although very low) to be successful when those requests happen simultaneously with the requests from the scheduled traffic. Therefore, first, we generate the distribution of the number of RA requests of scheduled devices within the synchronization range. The RA requests of H2H, low priority, high priority, and emergency will succeed when the number of RA requests of the scheduled devices is below the system capacity. We then calculate the percentage of the time p_t that the number of RA requests of the scheduled devices is below the capacity within the synchronization range. By combining this with the probability that the access requests from the scheduled devices do not appear, we obtain

$$\begin{aligned} P_{\text{LTE},v} = P_{\text{LTE},e} = P_{\text{LTE},l} = P_{\text{LTE},h} \\ = P_{\text{LTE},\text{bound}} + (1 - P_{\text{LTE},\text{bound}}) \times p_t. \end{aligned} \quad (3)$$

To estimate the access success probability of scheduled devices, let n be the index of the PRACH slots in the synchronization range and $f(n)$ be the probability that a UE makes the random access request at the n th PRACH slot within the synchronization range. $f(n)$ is then a probability mass function (PMF). Let $N_A = \delta_s \lambda_s$ be the total number of access requests in the synchronization range and $K = \delta_s N_{\text{PRACH}}$ be the number of PRACHs in the synchronization range, where λ_s is the number of RA requests per second for the scheduled traffic. Therefore, $f(n)N_A$ means the number of UEs that request for access at the n th PRACH slot. An example of $f(n)$ is shown in Fig. 5, which also

shows $f(n)N_A$ (the right y -axis), assuming $N_A = 35\,670$. The access success probability of scheduled traffic is then given by

$$P_{\text{LTE},S} = \sum_{n=1}^K \mathcal{I}(f(n)N_A \leq c) f(n) \quad (4)$$

where $\mathcal{I}(x)$ is the indicator function: $\mathcal{I}(x) = 1$ if x is true, and $\mathcal{I}(x) = 0$ otherwise. The reason that the summation instead of integration is used is because the PRACHs occur in discrete time. A more accurate approximation of the access success probability can be given by incorporating the success probability under different numbers of access requests (see Fig. 4), which can be obtained by running simulations. Let $p(x)$ be the access success probability when the number of access requests is x , then

$$P_{\text{LTE},S} = \sum_{n=1}^K p(f(n)N_A) f(n). \quad (5)$$

C. EAB

EAB is the state-of-the-art solution to the RAN overload problem [9]. Let us define $\text{EAB}(p_{\text{EAB}}, t_{\text{EAB}})$ as follows. A UE in the EAB barring class randomly selects a value between 0 and 1 every time before beginning the RA procedure. If the value is larger than p_{EAB} , the UE backs off for a period of time t_{EAB} and restarts the EAB process until a value smaller than p_{EAB} is selected.

First, let us consider the class of H2H, which is not barred (since we do not want the H2H traffic to be affected). Assume that when EAB is activated, the distribution of the random access requests of scheduled devices is reshaped as $f'(n)$. Let the total period that the number of random access requests is smaller than the capacity be t_o , i.e.,

$$t_o = \left\lceil \frac{1}{N_{\text{RACH}}} \right\rceil \times \sum_{n=1}^{\tau_r N_{\text{RACH}}} \mathcal{I}(f'(n)N_A \leq c) \quad (6)$$

where τ_r is the spreading range of $f'(n)$, and $\lceil \cdot \rceil$ is the ceiling function. *Spreading range* is the range that the number of access requests is nonzero after the reshaping of the access times. Note that it may happen (although with a very low probability) that the spreading range is infinite under this definition. If this happens, we can simply set a threshold for the number of access requests and get a good approximation. The access success probability of H2H is then given by

$$P_{\text{EAB},V} = \frac{t_o}{\tau_s} \quad (7)$$

which simply calculates the probability that the H2H traffic encounters the burst of the scheduled traffic with a number of access requests larger than the system capacity after the spreading.

The access success probability $P_{\text{EAB},E}$ of the class of emergency, which is not barred, can be also estimated similarly as in the case of H2H. Therefore, $P_{\text{EAB},E} = P_{\text{EAB},V}$.

Now, we discuss the access success probabilities of low- and high-priority traffic, which behave the same under EAB. Since the low- and high-priority traffic belong to the barred class in EAB, we need to consider the effect of barring to the access success probability due to exceeding the maximum delay constraint. The unsuccessful access probability due to barring is, thus

$$P_{o,l,\text{barring}} = (1 - p_{\text{EAB}})^{\lceil \gamma_l / t_{\text{EAB}} \rceil} \quad (8)$$

for low-priority traffic and

$$P_{o,h,\text{barring}} = (1 - p_{\text{EAB}})^{\lceil \gamma_h / t_{\text{EAB}} \rceil} \quad (9)$$

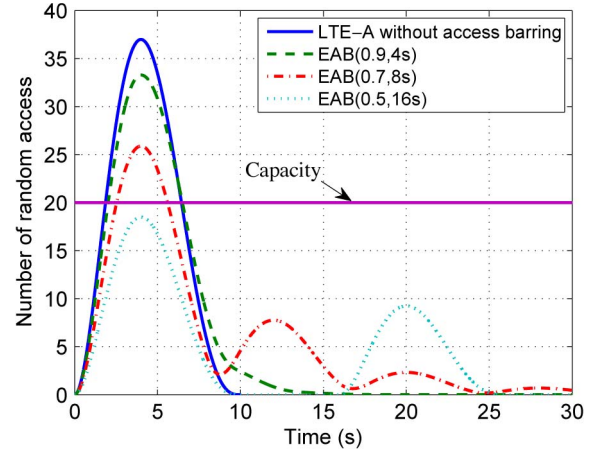


Fig. 6. Distribution of the number of random access requests of smart meters using LTE-A without access barring and EAB.

for high-priority traffic. Then, the access success probability is

$$P_{\text{EAB},L} \approx P_{\text{EAB},V} \times (1 - P_{o,l,\text{barring}}) \quad (10)$$

for low-priority traffic, and

$$P_{\text{EAB},H} \approx P_{\text{EAB},V} \times (1 - P_{o,h,\text{barring}}) \quad (11)$$

for high-priority traffic.

As before, the access success probability for scheduled traffic can be estimated as

$$P_{\text{EAB},S} = \sum_{n=1}^{\tau_r N_{\text{RACH}}} p(f'(n)N_A) f'(n). \quad (12)$$

D. PRADA

Here, we derive the access success probabilities when PRADA is applied.

Due to the prioritized virtual resource allocation, scheduled devices do not have impact on the random access requests of the classes of low priority and high priority. Although the *effective* capacity (due to the dedicated resource allocation) is lower, it is possible to design the resource allocation such that $\lambda_l + \lambda_h < \eta C$, where η is the percentage that the PRACH slots are allocated to high-priority/low-priority traffic. Therefore, the success probabilities of low and high traffic $P_{\text{PRADA},L} = P_{\text{PRADA},H} = 1$ can be achieved by a proper design.

To estimate the access success probability of scheduled devices, we need to investigate DAB since DAB is mainly designed to solve the problem of massive access requests of the scheduled traffic. We ignore the effect of T_{reset} and T_{extra} and only focus on the transition between states. The idea of DAB can be regarded as an automatic enabling/disabling mechanism for controlling the access traffic—barring is only activated when needed, i.e., when the system detects the possible access failure due to overloading. Therefore, the enabling mechanism plays a major role, and the unsuccessful access requests happen when the system wrongly evaluates the current access load. Note that the disabling mechanism only affects the access delay and does not play a role for the access success probability. Since eNB estimates the system load using the number of successful access requests, i.e., the number of UEs that select unique preambles, an access failure happens when the system is in state II, and the estimated S_i is larger than β (DAB is disabled at this moment), but the number of access requests is larger than the corresponding N_i (see Fig. 2). Mathematically, by denoting $N_i = g(S_i)$ as the mapping between S_i

TABLE I

COMPARISON OF THEORETICAL AND SIMULATED ACCESS SUCCESS PROBABILITIES. THE VALUES AT THE LEFT-HAND SIDE ARE FROM SIMULATIONS, WHEREAS THE VALUES IN THE PARENTHESES ARE FROM THEORETICAL ANALYSIS. SEE [10] FOR SYSTEM SETUP AND PARAMETERS

	Emergency	H2H	High priority	Low priority	Scheduled
	Seismic alarms	Voice call	Hospital e-care	Fleet management	Smart meters
LTE-A	0.987 (0.985)	0.984 (0.985)	0.985 (0.985)	0.985 (0.985)	0.234 (0.2065)
EAB(0.9, 4s)	0.987 (0.985)	0.986 (0.985)	0.986 (0.985)	0.985 (0.985)	0.300 (0.2817)
EAB(0.7, 8s)	0.987 (0.9898)	0.990 (0.9898)	0.966 (0.9574)	0.967 (0.9574)	0.604 (0.5892)
EAB(0.5, 16s)	1.000 (1.000)	1.000 (1.000)	0.776 (0.739)	0.770 (0.750)	1.000 (1.000)
PRADA	0.996 (0.9979)	0.998 (0.9979)	1.000 (1.000)	1.000 (1.000)	0.939 (0.9384)

and N_i (the curve in Fig. 2), we obtain the access success probability of scheduled traffic, i.e.,

$$\begin{aligned}
 P_{\text{PRADA},S} &= 1 - \mathbb{P}[N_i > g(\beta)|N_i > g(\alpha), S_i > \beta] \\
 &= 1 - \frac{\mathbb{P}[N_i > g(\beta), N_i > g(\alpha), S_i > \beta]}{\mathbb{P}[N_i > g(\alpha), S_i > \beta]} \\
 &= 1 - \frac{\mathbb{P}[N_i > g(\beta), S_i > \beta]}{\mathbb{P}[N_i > g(\alpha), S_i > \beta]} \\
 &= 1 - \mathbb{P}[N_i > g(\beta)|S_i > \beta]\mathbb{P}[N_i > g(\alpha)|S_i > \beta] \quad (13)
 \end{aligned}$$

where $\mathbb{P}[N_i > g(\beta)|S_i > \beta]$, and $\mathbb{P}[N_i > g(\alpha)|S_i > \beta]$ can be derived by knowing

$$\begin{aligned}
 \mathbb{P}[S_i = s|N_i = n] &= \binom{M}{s} \left[\frac{n}{M} \left(1 - \frac{1}{M} \right)^{n-1} \right]^s \\
 &\quad \times \left[1 - \frac{n}{M} \left(1 - \frac{1}{M} \right)^{n-1} \right]^{M-s}. \quad (14)
 \end{aligned}$$

The access success probability of emergency traffic $P_{\text{PRADA},E}$ can then be calculated as

$$P_{\text{PRADA},E} = \frac{\delta_s}{\tau_s} \times P_{\text{PRADA},S} + \left(1 - \frac{\delta_s}{\tau_s} \right) \times 1 \quad (15)$$

which follows from the fact that the access requests of the scheduled devices only arrive in a bursty way. On average, the RA request of an emergency traffic co-occurs with the requests of scheduled traffics with probability δ_s/τ_s , as explained before. When this happens, the request of the emergency traffic has probability $P_{\text{PRADA},S}$ to succeed. When not co-occurring with the scheduled traffic (the probability is $1 - \delta_s/\tau_s$), the access request of the emergency traffic will always succeed.

It is expected that the success probability of H2H $P_{\text{PRADA},V}$ satisfies the conditions $P_{\text{PRADA},V} > P_{\text{PRADA},S}$ and $P_{\text{PRADA},V} > P_{\text{PRADA},E}$ since we have allocated more virtual slots for the H2H traffic. Therefore, we use

$$P_{\text{PRADA},V} \approx \max\{P_{\text{PRADA},E}, P_{\text{PRADA},S}\} \quad (16)$$

to estimate the access success probability of H2H. Since $P_{\text{PRADA},E} > P_{\text{PRADA},S}$, we obtain

$$P_{\text{PRADA},V} \approx P_{\text{PRADA},E}. \quad (17)$$

IV. ACCURACY OF THEORETICAL ANALYSIS

Here, we show the accuracy of the theoretical analysis by comparing with the simulation results. The system setup and the simulation parameters follow [10].

For $M = 54$, $\hat{N} = [\log(54/53)]^{-1} = 53.5$ and $c = 20.05$. If the PRACH appears every 5 ms, there are 200 PRACHs per second ($N_{\text{RACH}} = 200$), and the expected number of successful RA requests is about 4000 per second ($C = 4000$). Therefore, the system capacity is 20 per 5 ms or 4000 per second.

1) *LTE-A Without Access Barring*: First, let us consider the random access in LTE-A. The RA requests of H2H, low priority, and high priority will succeed since $\lambda_v + \lambda_e + \lambda_l + \lambda_h = 9 + 126 + 80 + 160 = 375$ is smaller than the system capacity of 4000 per second. Therefore, $P_{\text{LTE},V} = P_{\text{LTE},E} = P_{\text{LTE},L} = P_{\text{LTE},H} > P_{\text{LTE},\text{bound}} = 1 - \delta_s/\tau_s = 1 - 10/(5 \times 60) = 0.967$ [see (2)]. As stated earlier, we can consider the possibility of access success when competing with smart meters. Let $f(n)$ be the discretized beta distribution with parameters (3, 4). Fig. 6 shows the distribution of the number of RA requests of smart meters. The RA requests of H2H, low priority, high priority, and emergency will succeed when the number of RA requests of the smart meters is below 20 (the system capacity per 5 ms). During the period of 10 s, the number of RA requests of the smart meters is below 20 in 54.2% of the PRACH slots. By combining this with the probability that the RA requests from the smart meters do not appear, we obtain $P_{\text{LTE},V} = P_{\text{LTE},E} = P_{\text{LTE},L} = P_{\text{LTE},H} = P_{\text{LTE},\text{bound}} + (1 - P_{\text{LTE},\text{bound}}) \times p_t = 0.967 + 0.033 \times 0.542 = 0.985$ [see (3)]. To estimate the access success probability of smart meters, by plugging in the values to (4) or (5), we obtain $P_{\text{LTE},S} = 0.2065$.

2) *EAB*: Now, we consider the random access under EAB. In Fig. 6, the distribution of the random access requests of smart meters is reshaped by EAB(0.9, 4 s). As shown in Fig. 6, the period that the number of access requests over the capacity 20 is 4.48 s. Therefore, $P_{\text{EAB},V} = P_{\text{EAB},E} = (300 - 4.48)/300 = 0.985$ [see (7)]. When EAB(0.7, 8 s) is used, in Fig. 6, the period that the number of access requests is over the capacity 20 is 3.07 s. Therefore, the access success probability of H2H is $P_{\text{EAB},V} = P_{\text{EAB},E} = (300 - 3.07)/300 = 0.9898$. After the EAB(0.5, 16 s) is used, the number of RA requests is always under the system capacity. Thus, $P_{\text{LTE},V} = P_{\text{EAB},E} = 1$. For the traffics of low priority and high priority, when EAB(0.9, 4 s) is used, the outage probability due to barring is $0.1^{\lceil 20/4 \rceil} = 0.1^5 = 0.00001$ (since the maximum delay constraint is 20 s). Therefore, $P_{\text{EAB},L} = P_{\text{EAB},H} \approx 0.985 \times (1 - 0.00001) \approx 0.985$ [see (10) and (11)]. When EAB(0.7, 8 s) is used, the outage probability due to barring is $0.3^{\lceil 20/8 \rceil} = 0.3^3 = 0.027$. Then $P_{\text{EAB},L} = P_{\text{EAB},H} \approx 0.985 \times (1 - 0.027) = 0.9574$. For the case of EAB(0.5, 16 s), the outage probability due to barring is $0.5^{\lceil 20/16 \rceil} = 0.5^2 = 0.25$. Thus, $P_{\text{EAB},L} = P_{\text{EAB},H} \approx 0.985 \times (1 - 0.25) = 0.739$. For smart meters, by using (12), we can calculate that $P_{\text{EAB},S} = 0.2817$, $P_{\text{EAB},S} = 0.5892$, and $P_{\text{EAB},S} = 1$ when using EAB(0.9, 4 s), EAB(0.7, 8 s), and EAB(0.5, 16 s), respectively.

3) *PRADA*: When using PRADA, $P_{\text{PRADA},L} = P_{\text{PRADA},H} = 1$ since the system capacity of 400 (derived from $1/10 \times 4000$) is still larger than the sum of the number of the random access requests $80 + 160 = 240$ for the classes of low priority and high priority (although now, the capacity is only 1/10 of the original capacity). By using (13) and (14), we obtain $P_{\text{PRADA},S} = 0.9384$. Then, $P_{\text{PRADA},E} = 10/300 \times 0.9384 + 290/300 \times 1 = 0.9979$ from (15). Finally, $P_{\text{PRADA},V} \approx \max\{P_{\text{PRADA},E}, P_{\text{PRADA},S}\} \approx P_{\text{PRADA},E} = 0.9979$ from (16) and (17).

The results of theoretical analysis are summarized in Table I to compare with the simulation results. This leads to the conclusion that the theoretical analyses and the simulations match very well.

V. CONCLUSION

In this paper, the PRADA framework for solving the RAN overload problem in 3GPP LTE-A networks due to MTC has been analyzed. We have mathematically derived and compared the access success probabilities of systems applying EAB and the PRADA framework. The theoretical analyses have been shown to match the simulation results very well.

APPENDIX

The problem of deriving the expected number of successful RA requests per PRACH slot can be formulated as a bins-and-balls problem. Let Y be the number of preambles that are chosen exactly by one UE and X_i , $i = 1, \dots, M$, be indicators that if the i th preamble is chosen exactly once, $X_i = 1$; otherwise, $X_i = 0$. Then, $Y = X_1 + X_2 + \dots + X_M$. By taking expectation on both sides, $\mathbb{E}[Y] = \mathbb{E}[X_1 + X_2 + \dots + X_M] \stackrel{(a)}{=} \mathbb{E}[X_1] + \mathbb{E}[X_2] + \dots + \mathbb{E}[X_M] \stackrel{(b)}{=} M\mathbb{E}[X_1]$, where (a) follows from the linearity property, and (b) is due to $\mathbb{E}[X_1] = \mathbb{E}[X_2] = \dots = \mathbb{E}[X_M]$. For each UE, preamble 1 has probability $1/M$ of being chosen, and only one out of N UEs chooses preamble 1. Therefore, $\mathbb{E}[X_1] = (N/M)(1 - 1/M)^{N-1}$. Finally, $\mathbb{E}[Y] = N(1 - 1/M)^{N-1}$.

REFERENCES

- [1] L. Atzori, A. Iera, and G. Morabito, "The Internet of Things: A survey," *Comput. Netw.*, vol. 54, no. 15, pp. 2787–2805, Oct. 2010.
- [2] D. Niyato, L. Xiao, and P. Wang, "Machine-to-machine communications for home energy management system in smart grid," *IEEE Commun. Mag.*, vol. 49, no. 4, pp. 53–59, Apr. 2011.
- [3] K.-C. Chen, "Machine-to-machine communications for healthcare," *J. Comput. Sci. Eng.*, vol. 6, no. 2, pp. 119–126, Jun. 2012.
- [4] Z. Fadlullah, M. Fouda, N. Kato, A. Takeuchi, N. Iwasaki, and Y. Nozaki, "Toward intelligent machine-to-machine communications in smart grid," *IEEE Commun. Mag.*, vol. 49, no. 4, pp. 60–65, Apr. 2011.
- [5] M.-Y. Cheng, G.-Y. Lin, H.-Y. Wei, and A.-C. Hsu, "Overload control for machine-type-communications in LTE-advanced system," *IEEE Commun. Mag.*, vol. 50, no. 6, pp. 38–45, Jun. 2012.
- [6] A. Ksentini, Y. Hadjadj-Aoul, and T. Taleb, "Cellular-based machine-to-machine: Overload control," *IEEE Network*, vol. 26, no. 6, pp. 54–60, Nov./Dec. 2012.
- [7] A. Gotsis, A. Lioumpas, and A. Alexiou, "M2M scheduling over LTE: Challenges and new perspectives," *IEEE Veh. Technol. Mag.*, vol. 7, no. 3, pp. 34–39, Sep. 2012.
- [8] S.-Y. Lien, K.-C. Chen, and Y. Lin, "Toward ubiquitous massive accesses in 3GPP machine-to-machine communications," *IEEE Commun. Mag.*, vol. 49, no. 4, pp. 66–74, Apr. 2011.
- [9] *R2-113650: Report of 3GPP TSG WG2 Meeting No.73bis*, 3GPP TSG WG2, Apr. 2011.
- [10] J.-P. Cheng, C.-H. Lee, and T.-M. Lin, "Prioritized random access with dynamic access barring for RAN overload in 3GPP LTE-A networks," in *Proc. IEEE GLOBECOM Workshops*, Dec. 2011, pp. 368–372.
- [11] *Evolved Universal Terrestrial Radio Access (E-UTRA) Medium Access Control (MAC) Protocol Specification*, 3GPP TS 36.321 V10.0.0, Dec. 2010.

On the Bit Error Probability of Optimal Multiuser Detectors in Cooperative Cellular Networks

Rajitha Senanayake, *Student Member, IEEE*,
Phee Lep Yeoh, *Member, IEEE*, and Jamie S. Evans, *Member, IEEE*

Abstract—In this paper, we present new theoretical analysis on the uncoded bit error probability (BEP) of optimal multiuser detectors in cooperative cellular networks. We consider the uplink of a cooperative network where an arbitrary number of receivers jointly detect the signals transmitted from multiple transmitters. For such a network, we derive accurate upper and lower bounds on the BEP with independent Rayleigh fading and arbitrary path loss. We observe that our lower bound accurately approximates the BEP at low signal-to-noise ratios (SNRs), whereas the upper bound is accurate at high SNRs. We further evaluate our bounds asymptotically to explicitly characterize the cooperative diversity order and array gains in the high-SNR regime.

Index Terms—Base station cooperation, bit error probability (BEP), multiuser detection.

I. INTRODUCTION

A major barrier in realizing theoretical minimum error rates for uplink transmission in cellular networks is intercell interference [1]. The conventional approach to manage intercell interference is to adopt a sparse frequency reuse pattern such that users in neighboring cells communicate over orthogonal frequency bands. This is problematic in dense network areas (e.g., commercial districts and city centers) where the capacity requirement is very high. Base station cooperation is a promising approach to exploit interference by treating antennas of multiple cells as a virtual multiple antenna array [2], [3]. In so doing, base station cooperation effectively treats intercell interference as useful information and significantly improves the network reliability and spectral efficiency.

The concept of a joint processing global receiver that has access to all the received signals was initially proposed in [4] and [5]. The Wyner model in [4] was further extended to incorporate more realistic characteristics in cellular networks such as fading [6] and finite-capacity backhaul links [7]. Considering the bit error probability (BEP), a belief propagation algorithm for base station cooperation was proposed in [8], where local message passing was shown to provide a globally near-optimum error rate. Recently, an upper bound on the symbol error probability (SEP) of cooperative cellular networks has been considered in [9], where a union bound on the SEP is derived by adding the pairwise error probabilities over all possible transmit–receive symbols. The results were valid for distinct path-loss values between the transmitters and the receivers.

In this paper, we present new theoretical analysis on the BEP of cooperative base stations for both binary phase-shift keying (BPSK) and quadrature phase-shift keying (QPSK). We consider the uplink of a cooperative cellular network with an arbitrary number of transmitters

Manuscript received April 22, 2013; revised August 22, 2013 and October 29, 2013; accepted November 6, 2013. Date of publication November 27, 2013; date of current version June 12, 2014. The review of this paper was coordinated by Prof. H.-F. Lu.

R. Senanayake and P. L. Yeoh are with the Department of Electrical and Electronic Engineering, University of Melbourne, Parkville, Vic. 3010, Australia (e-mail: r.senanayake@student.unimelb.edu.au; phee.yeoh@unimelb.edu.au).

J. S. Evans is with the Department of Electrical and Computer Systems Engineering, Monash University, Clayton, Vic. 3800, Australia (e-mail: jamie.evans@monash.edu).

Digital Object Identifier 10.1109/TVT.2013.2293141